

The Polarisation Signatures of Microlensing

A.M. Newsam ^{a,1} J.F.L. Simmons ^b, M.A. Hendry ^b,
I.J. Coleman ^{b,2}

^a*Department of Physics and Astronomy, University of Southampton,
Southampton, UK*

^b*Department of Physics and Astronomy, University of Glasgow, Glasgow, UK*

Abstract

It has already been shown that microlensing can give rise to a non-zero variable polarisation signal. Here we use realistic simulations to demonstrate the additional information that can be gained from polarimetric observations of lensing events.

Key words: Polarisation, Gravitational lensing, Stars:Atmospheres

1 Introduction

It has been shown by Simmons, Newsam & Willis (1995) (hereafter SNW95) that microlensing of stars can produce a distinctive and significant polarisation signature, even for lensed stars with no net unamplified polarisation. In this contribution, we use the model developed in SNW95 to simulate a series of realistic observations of microlensing events. We use these simulations to examine how much additional information about the parameters of the lensing event can be determined from polarisation measurements.

2 Microlensing induced polarisation of unpolarised stars

Normally, the light received from stars is unpolarised unless the star has some suitable asymmetry (eg an asymmetric wind or radial distortion). However,

¹ E-mail: amn@astro.soton.ac.uk

² Current address: British Antarctic Survey, Cambridge, CB3 0ET, UK

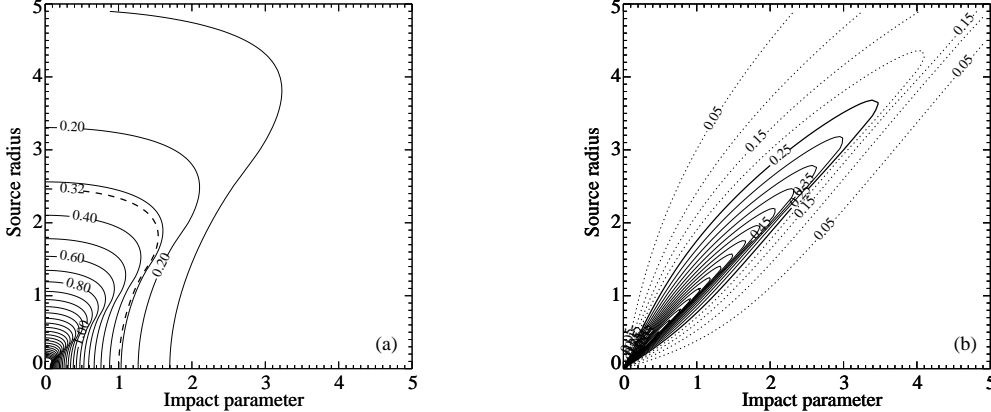


Fig. 1. Flux amplification and polarisation for microlensing of a simple stellar model. Both figures show the results for a range of source radii and impact parameters d_0 , both in units of the angular einstein radius. Figure (a) shows the photometric amplification with contours spaced by 0.1 magnitudes. The dashed contour is for an amplification of 0.32 mag – that expected in the point-source approximation with $d_0 = 1$. Figure (b) shows the percentage polarisation observed. Contours are at intervals of 0.05% with dashed contours below 0.25%.

the emission from the limb of the star can be expected to be quite strongly polarised. Therefore, during a microlensing event, different parts of the limb may be amplified by different amounts, breaking the symmetry of the star and giving rise to an observable net polarisation.

This effect will be most significant if the stellar radius is comparable to or larger than the einstein radius of the lens projected onto the plane of the lensed star. The observed polarisation will reach a maximum as the line of sight to the lens crosses the limb of the star. This gives rise to the distinctive polarisation profiles of lensing events given in SNW95, with a polarisation peak coincident with the amplification peak if the line of sight to the lens remains outside the stellar disk, but a double-peaked polarisation profile if the lens appears to cross the disk of the star (“transit” events).

Clearly, when studying an actual lensing event, one would use a model appropriate to the observed stellar type. Also, one would hope to be able to obtain information about the lensed star itself, as well as the parameters of the lensing event (e.g. Valls-Gabaud 1998, Coleman et al 1997). However, here we will only consider the lensing parameters themselves and so we consider a simple “generic” stellar atmosphere model. The full details of the models we use for the stellar atmosphere and microlensing event are given in SNW95.

Figure 1 shows the results of applying a lensing amplification function to this model for a range of source/lens configurations. As shown in SNW95, when the source radius R is very much less than the projected distance between the star and the lens (the impact parameter d_0), the star is effectively a point

source and there is no measurable polarisation. However, when $R \lesssim d_0$, significant polarisation can occur, and the flux amplification is modified from that expected for the point-source approximation (see also Gould 1994, Witt & Mao 1994).

3 Simulations of realistic observations

Using this model, we have simulated photometric and polarimetric observations of microlensing events with realistic sampling and errors. Two such simulations are given here (selected at random from our “catalogue”). Both simulations are for a $V=17$ star in the LMC lensed by a $0.01 M_\odot$ lens at half the distance to the LMC with a velocity on the plane of the sky of 50 km/s. The impact parameter in both cases is 0.1 angular einstein radii. Observations are taken once “nightly”. Photometric errors are based on Udalski et al (1994) and polarimetric errors are calculated for a 2-hour exposure in V on a 1.2m telescope. The first simulation is for an $R = 100R_\odot$ source (figure 2, left - a transit) and the second for $R = 10R_\odot$ (figure 2, right). The figure also shows the results of χ^2 fits to the simulated data for two interesting parameters (the stellar radius R and the impact parameter d_0). In both cases, the inclusion of polarimetric data provides a strong constraint on the fit. In particular, in the $10R_\odot$ case, where the polarisation measurements are only just significant at the maximum amplification, there is still useful information for determining the stellar radius.

4 Conclusions

We have shown that microlensing can produce a significant, distinctive polarisation signature and that observations of these signatures can provide considerable additional information about the parameters of a lensing event. In particular, some of the degeneracy between the various parameters of the lensing event present in purely photometric observations can be broken. The realistic simulated observations presented here demonstrate that such observations can be obtained with modest resources. In a future paper (Newsam et al, in preparation) we will present a thorough exploration of the lensing parameter-space with more realistic stellar atmosphere models both to determine when polarisation measurements would be most useful, and to examine the use of such measurements to study the atmosphere of the *lensed* star (see Coleman et al 1997).

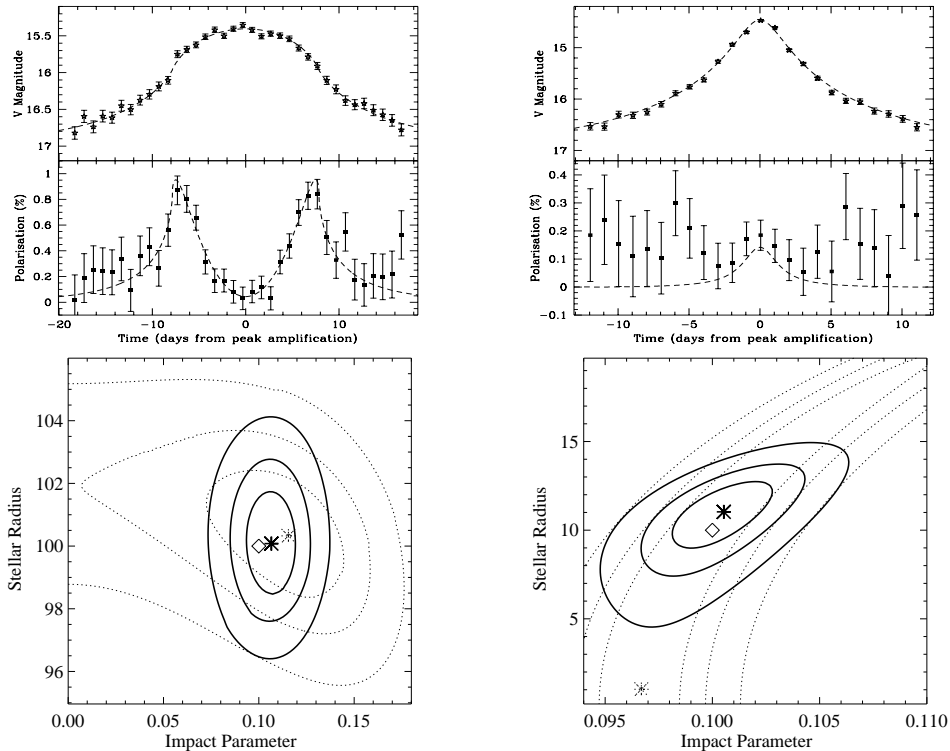


Fig. 2. Simulated observations and fits. The upper panels show the model photometric and polarimetric profiles and the simulated observations. The lower panels show the χ^2 surfaces of two fits to the data. The thicker, solid contours and star show the χ^2 surface and best fit results for a fit to both the flux and polarimetric data simultaneously. The dashed lines and star show the result of a fit to just the photometric data. The diamond shows the true solution. Contours are 68%, 95% and 99.7% confidence regions. The left-hand panels are for an $R = 100R_{\odot}$ star, the right-hand panels for $R = 10R_{\odot}$. It should be noted that the fit actually gives the stellar radius in units of the angular einstein radius, but this has been converted to Solar radii for clarity.

References

- Coleman, I.J., Simmons, J.F.L., Newsam A.M. & Bjorkmann, J.E., 1997, in “Variable stars and astrophysical returns of microlensing surveys”, eds R. Ferlet et al.
- Gould, A., 1994, ApJ, 421, L71.
- Simmons, J.F.L., Newsam, A.M. & Willis, J.P., 1995, MNRAS, 276, 182 (SNW95).
- Udalski, A. et al, 1994, Acta. Astron., 44, 165.
- Valls-Gabaud, D., 1998, MNRAS (in press).
- Witt, H.A. & Mao, S. 1994, ApJ, 430, 505.